CHARACTERIZATION OF CRITICAL STRETCH RATE USING OUTWARDLY PROPAGATING SPHERICAL FLAMES

Daniel DE LA ROSA-URBALEJO [*], ***Simón MARTÍNEZ-MARTÍNEZ, Fausto A. SÁNCHEZ-CRUZ***

Universidad Autónoma de Nuevo León, Facultad de Ingeniería Mecánica y Eléctrica (FIME), Laboratory for Research and Innovation in Energy Technology (LIITE), Nuevo León, México.

*Corresponding author; E-mail: daniel.delarosarb@uanl.edu.mx

Outwardly propagating spherical flames within a constant volume combustion chamber (CVCC) are studied to analyse the non-linear relationship between flame stretch and flame speed, enabling a critical appraisal of a methodology proposed for characterizing the critical stretch rate. Four fuels, namely methane, propane, methanol and ethanol in air, are chosen to investigate the correlation between maximum critical stretch rate and the flame extinction across a range of equivalence ratios at various ambient conditions in under-driven flames, and to compare the hypothesis against data from the traditional counter-flowing flame technique. Flame propagation is recorded via high-speed Schlieren photography, and low ignition energies are achieved via a variable capacitive-discharge supply, enabling the critical early stages of flame propagation, critical stretch rate and the sensitivity of the non-linear methodology to ignition energy to be systematically analysed. The non-linear methodology shows partial agreement with extinction stretch rate from counter flowing flames, particularly in the case of gaseous fuels. Although the fuel vapour data lies between previous extinction stretch rate measurements using the counter-flowing flame methodology, and predictions from chemical kinetic schemes, a 40% deviation is observed. A mathematical expression was produced to determine the critical stretch at the specific conditions of the present work.

Key words*: laminar burning velocity, liquid fuels, gaseous fuels, premixed flames, critical stretch rate, extinction stretch rate.*

1. Introduction

Operational issues resulting from fuel variability and combustor flexibility necessitate detailed research in the fundamental aspects of combustion control [1-3]. The study of extinction stretch rates (K_{ext}) is key for the reduction of pollutants formed from turbulent flames, prevailing within power or propulsion systems, and preventing extinction by stretch [4, 5]. Taking the gas turbine industry as an example, extinction tests are usually required to determine a wide range of operational conditions with high levels of combustion efficiency [6, 7], and for the validation of chemical kinetic mechanisms [8, 9].

Measurements of extinction stretch rate are traditionally undertaken in counter-flowing burners [1, 2, 4, 8, 10-12], however it has been suggested that an outwardly-propagating spherical flame configuration (with low ignition energy) [13, 14] could provide an alternative method of measurement. This technique consists of approximating K_{ext} as the highest corresponding stretch rate experienced by the spherical flame, prior to acceleration with decreasing stretch. This is assuming that propagation follows the non-linear trend between stretched flame speed and stretch rate [15]. For clarity, and to differentiate each parameter in discussion, this point is herein denoted as the critical stretch rate (α_{Cr}).

The aim of this work is to appraise the hypothesis that α_{Cr} is quantitatively equivalent to K_{ext} as quoted in the literature for counter-flow burners [16] proposed critical radius as the radius above which an ignition kernel can lead to a successful ignition. This work thus presents analysis and discussion of experiments undertaken with four fuels (two gaseous, and two pre-vaporised liquids) namely methane, propane, methanol and ethanol (CH_4, C_3H_8, CH_3OH, and C_2H_5OH), with measured values of α_{Cr} benchmarked against corresponding published values of K_{ext} derived using the counter-flow technique. It is worthy to note that the same analysis followed in the present work can be applied also to biodiesel and biogas, among others, fuels commonly used in internal combustion engines [17-19]. For an outwardly propagating spherical flame to exhibit the non-linear characteristic beyond the critical point (α_{Cr}), flame propagation has to be both ignited with a low enough energy to minimise spark influence and flame thickness effect [20] on the early stages flame growth and heavily influenced by stretch. As such results are presented at conditions where these sensitive measurements are possible and the curvilinear trend is evident in the raw measured data.

It is important to note that the effects of ignition energy and mixture Lewis number (*Le*) on the flame kernel growth in a spherical flame by allowing for strongly stretched flames was comprehensively investigated theoretically and experimentally elsewhere [16, 20, 21]. Their results showed that there is a critical flame radius, above which both the linear and non-linear extrapolation for flame speeds are valid. Moreover, they suggested that this critical radius is the point past which a kernel can fully propagate as a successful ignition; however, no comparisons of the corresponding stretch rate value against extinction stretch rates were reported.

2. Experimental Methodology

The CVCC employed for this investigation is presented in Fig. 1. The cylinder has an internal diameter of 0.26 m (34.8 L), with 4 diametrically opposed 0.1 m quartz viewing windows. Following evacuation of the chamber, precise masses of liquid fuels (graded ≥99.9%) are introduced to the chamber via syringe, through a self-sealing septa housing. Gaseous fuels are introduced through a manifold with fine needle valve control. When required conditions are met, combustion is initiated. Confinement effects are minimized by limiting the use flame radii to 8% of the vessel radius [22].

By employing a Schlieren optical setup, the system generates an image of the working area. A 50W light source was used with a 0.1 m diameter converging mirror to provide the collimated parallel light, directed through the test section. This beam is then refocused using an identical second mirror onto a knife-edge aperture (focal length 0.94 m). The refracted portion of the beam unblocked by the edge focuses imperfectly, thereby creating light intensity gradients. These produce edges used to identify the isotherm representative of the flame front boundary, which are visually recorded using the aforementioned camera. Images are then exported to a bespoke data processing script, which outputs flame-edge positional data, with a resolution of ~0.14 mm per pixel.

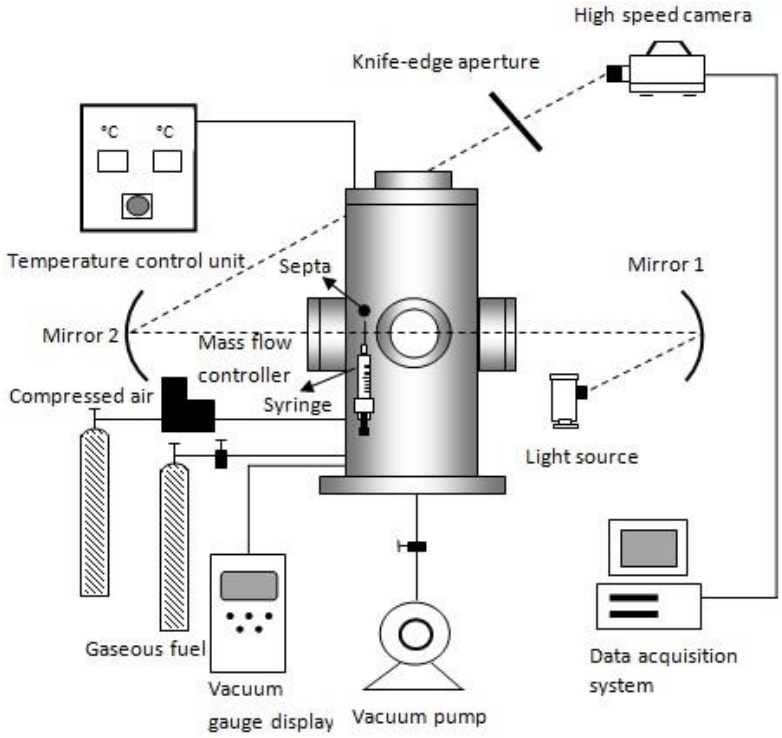

Figure 1. Schematic setup of the cylindrical constant volume combustion chamber (CVCC).

A variable energy capacitive-discharge ignition system is used to ignite the reactant mixture, with a full description is presented elsewhere [23, 24]. The circuitry contains three 0.47 μF rapid-discharge capacitors, with a variable voltage power supply (0-350V). Using Eq. 1, a theoretical energy of 0-85 mJ is provided as a function of system voltage (V) and capacitance (C).

$$E = \frac{CV^2}{2} \tag{1}$$

3. Theory and Analysis

The technique adopted is a well-documented methodology for the determination of flame front position, and as such has been used by several authors [5, 13-15, 25-30] to measure optically the propagation of spherical flames. The stretched flame speed (S_n) is obtained as the measured differential of Schlieren flame front radius (r_{sch}) and time (t), simply:

$$S_n = \frac{dr_{sch}}{dt} \tag{2}$$

For an outwardly propagating spherical flame of area (A) without the occurrence of cellular structure, the flame stretch rate (α) can be simplified as:

$$\alpha = \frac{1}{A}\frac{dA}{dt} = \frac{2}{r_{sch}}\frac{d_{rsch}}{dt} = \frac{2}{r_{sch}}S_n \tag{3}$$

A linear relationship between stretch and flame speed is presented, where the gradient defines the burned gas Markstein length (L_b):

$$S_L - S_n = L_b\alpha \tag{4}$$

The unstretched flame speed (S_L) is obtained as the extrapolated intercept value of S_n at $\alpha = 0$. However, this linear relationship is the result of several assumptions, which can lead to an

overestimation of derived S_L in some conditions [31]. The relationship proposed by Kelly and Law [15] takes into account the non-linearity of S_n against α when the flame is heavily influenced by stretch, and is given in Eq. 5.

$$\left(\frac{S_n}{S_L}\right)^2 \ln\left(\frac{S_n}{S_L}\right)^2 = -\frac{2L_b\alpha}{S_L} \tag{5}$$

At constant pressure the unstretched laminar burning velocity (u_L) is obtained from S_L by applying the density ratio of burned (ρ_b) and unburned gases (ρ_u); given by Eq. 6.

$$u_L = S_L\left(\frac{\rho_b}{\rho_u}\right) \tag{6}$$

In the context of this work there are several scenarios resulting from spark influence on stretched flame propagation; on one hand, when energy is low, the apparent acceleration falls then increases as propagation is fully established with decreasing stretch. Conversely, an increase in spark energy can lead to an enhanced initial flame speed due to higher level of heat release [27]. This is exacerbated when the flame is less influenced by stretch, minimum ignition energy is low, and the heat release rate from the flame is enhanced. Therefore whenever the association given in Eq. 5 is fitted or plotted to attain u_L, a safety factor was included, choosing 10 mm as the minimum flame radius for observation in this study. Additionally, in order to minimize radiation uncertainty, flame radii were limited to <2cm [22].

4. Results

4.1. Critical stretch rate (α_{Cr})

The effect of ignition energy on early flame development and the relationship with stretch rate are now considered in detail. Experiments were conducted employing a range of spark energies to assess the influence on subsequent flame evolution at high stretch rates (small radii).

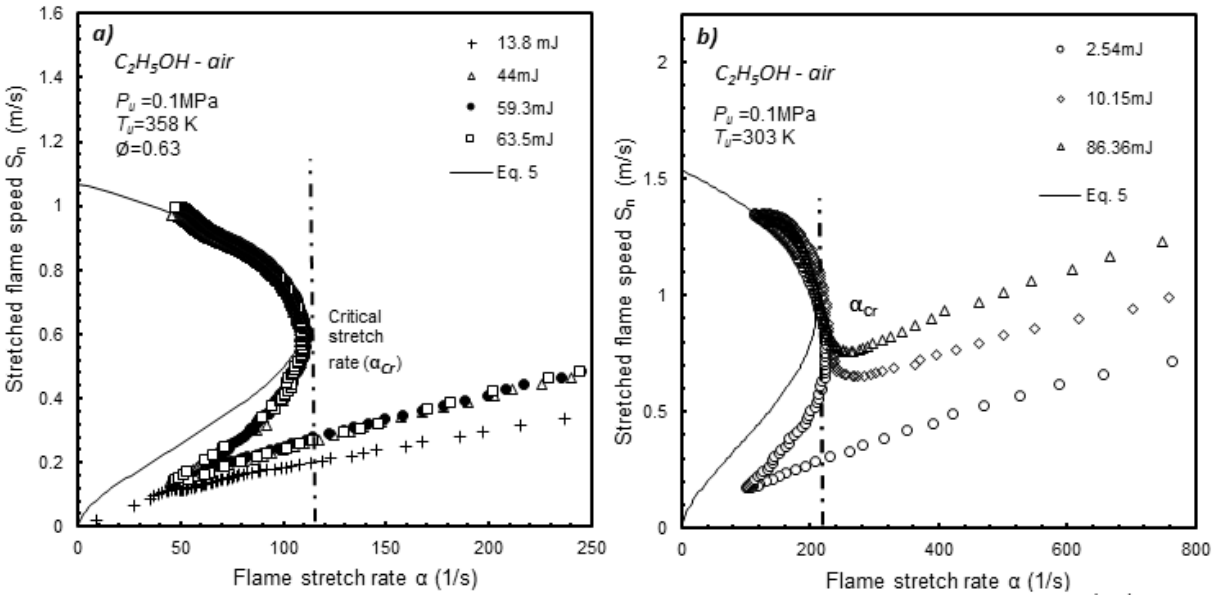

Figure 2. a) Lean ethanol flame propagation at 0.1 MPa and 358 K, with change in ignition energy, and b) Lean ethanol flame propagation at 0.1MPa and 303K, with change in ignition energy.

Figure 2a shows the influence of ignition energy on the early stages of flame propagation. Lean ethanol mixtures have been used to demonstrate the observed trends, as ethanol requires relatively higher ignition energy to initiate combustion with the corresponding propagation more influenced by stretch. It is seen in Fig. 2 that an initial linear trend is observed in the region of highest stretch-rate (lower right in plots) which is an ignition effect as has been discussed by previous authors [16, 32], and is thus removed from the derivation of critical stretch rate by taking adopting a minimum radius of 10 mm for which data is valid for the required data fit.

As can be seen in the case of ultra-lean ethanol flame (Fig. 2) by reducing the ignition energy too low (13.8 mJ) a non-self-propagating flame kernel that did not provide sufficient heat release in relation to the diffusion resulted, causing a marginally lower flame speed in relation to stretch rate, and hence flame extinguishment, before the first turning point could be achieved. According to Chen et al. [20] this flame reverse is provoked by the substantial flame thickening of the flame initiated by the lowest ignition energy before it reaches the maximum Karlovitz number (*Ka*).

In Figure 2b, data is presented for ethanol-air at an increased equivalence ratio of 0.75 and a reduced initial temperature of 303K, this combination allowed a lowering of the minimum ignition energy, for self-propagating flames due to an increase in the flame temperature and heat release. Decreasing the ignition energy induces a clear change in the development of the stretched flame; however, it was observed that there was little difference in the fitted non-linear extrapolation equation if the aforementioned minimum 10 mm radius was applied for the relevant measurement points.

It was observed that the overdriven flames witness at 10 and 86 mJ disguise the critical turning point, as has been observed by other authors [15, 27] emphasising the critical influence of low ignition energies in the application of this experimental methodology. Hence, in these cases where significant over driving of the flame witnessed it was necessary to apply data-fitting and extrapolation to approximate α_{Cr}. In the case of further increased equivalence ratio even very low ignition energies overdrive the flame past this point, hence direct measurement of α_{Cr} is no longer viable meaning the extrapolation method must be adopted.

The following sections provide comparisons between the empirical α_{Cr} values obtained in this study at a range of different equivalence ratios, perceived to exasperate the effects of flame stretch and corresponding published K_{ext} values from counter-flowing flames using the counter-flowing flame methodology. Data points from the measured flame trajectory have been used to present the measured α_{Cr} values if possible, however in the case of mixtures that had to be slightly overdriven, to achieve repeatable combustion then the value extrapolated from the non-linear extrapolation equation is presented, with the difference between measured and extrapolated data is identified on each graph.

4.1.1 Methane/air

A comparison between values of α_{Cr} calculated in the present work, and K_{ext} from [33] and [2] is shown in Fig. 3 for a) rich and b) lean mixtures, respectively. In their respective works the authors utilise a single-flame configuration, which is preferred to the symmetric twin flame which is susceptible to instabilities, affecting both topology and response.

Complete non-linear flame trajectories are observed for Ø = 1.3 – 1.4 only in this study, and so the non-linear extrapolation equation is used to provide all further values as presented by white diamonds. As can be seen in Fig. 3 there is good agreement in the extinction stretch rate characteristics proposed by both methodologies for rich flames with a strongly correlating trend with both the measured

and extrapolated data, however it is noted that there is a larger variance near the peak burning velocity around Ø = 1.1.

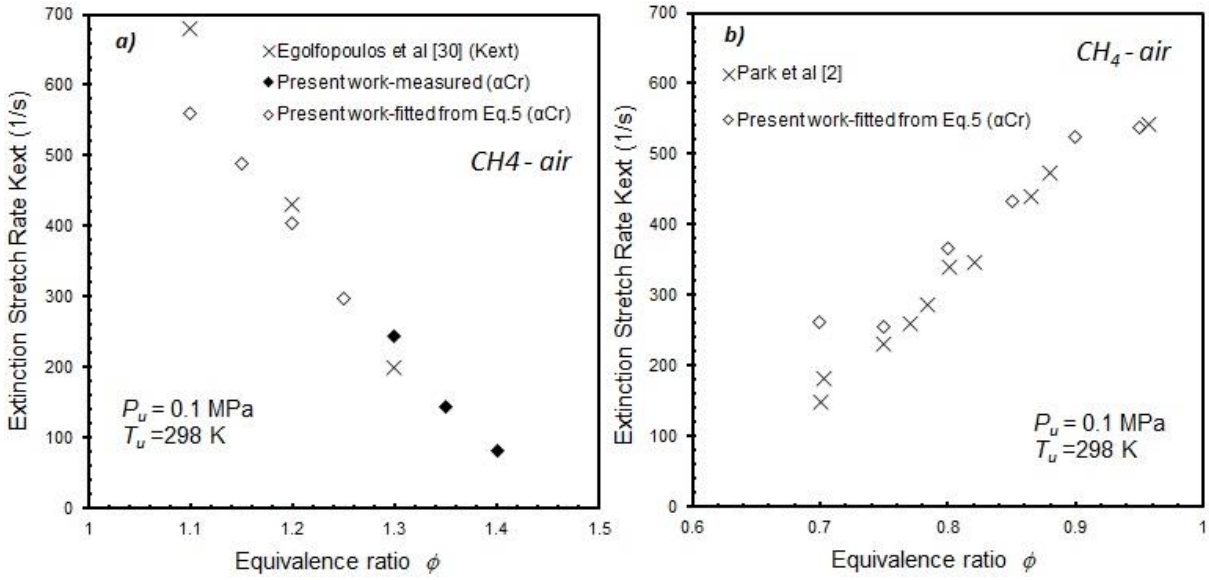

Figure 3. Comparison of experimental α_{Cr} against K_{ext} for a) rich and b) lean CH_4/air mixtures at 0.1 MPa and 298 K.

4.1.2 Propane/air

Lean propane/mixtures, α_{Cr} examined in the present work are compared to those obtained to values of K_{ext} taken from the results from [10] in Fig. 4. As can be seen for Ø = 0.65 to 0.75 full non-

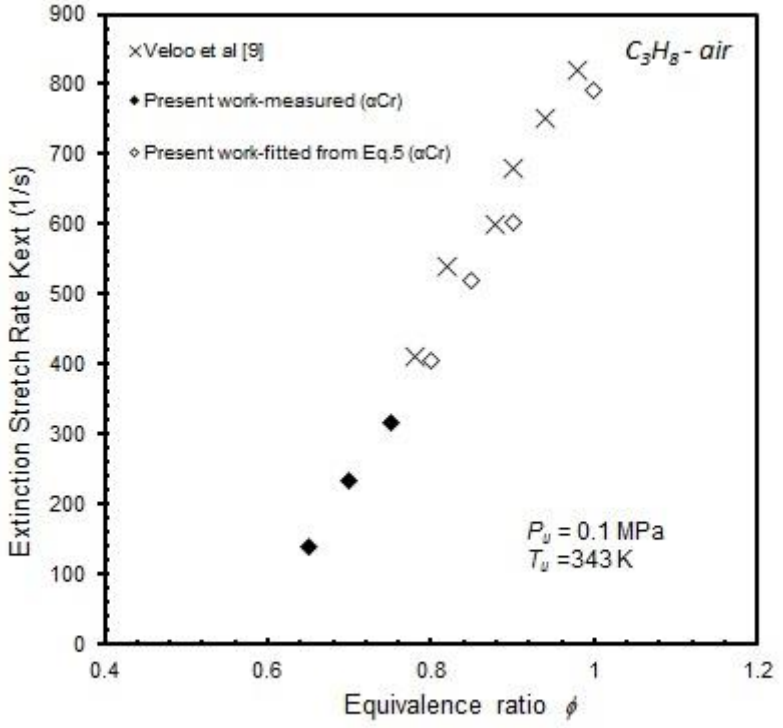

Figure 4. Comparison of experimental α_{Cr} against K_{ext} for lean C_3H_8/air mixtures at 0.1 MPa and 343 K.

linear flame trajectories are observed and values of α_{Cr} can be measured directly. For Ø = 0.8 – 1.0, flames are readily overdriven, requiring α_{Cr} values to be derived using the non-linear extrapolation equation.

It is observed that the measured values of α_{Cr} increase with equivalence ratio, following the same trends exhibited by data presented by Veloo et al. [10]. As for the methane/air data, propane/air systems exhibit good agreement with those obtained using counter-flow burners. Hence, for the two lower chain gaseous hydrocarbon fuels tested, α_{Cr} provides a good approximation of K_{ext}.

Now the hypothesis of the present work is applied to the fuel vapour of two alcohols currently being proposed as sustainable energy alternatives to conventional fuels namely Methanol and Ethanol.

4.1.3 Methanol – air and Ethanol – air flames

Figure 5a shows the comparison between α_{Cr} obtained from the present work and K_{ext} from Holley et al. [8] for lean methanol/air mixtures.

Results obtained in the present study show an offset from experimentally derived counter-flow data presented by Holley et al. [8], although both datasets demonstrate a similar trend in terms of change in stretch rate with equivalence ratio. One explanation for this offset could be inaccuracies in equivalence ratio which are notoriously harder to control in the case of liquid vapours compared with gaseous fuels, due to issues with complete evaporation and potential 'dewing' out of liquid fuels on any surface that are cooler than the saturation temperature of the vapour in question.

Furthermore, the experimental results derived in this study are closer to the trend lines predicted by published chemical kinetic schemes HD98, LDH03, and FDC00as presented by Holley et al. [8]. As can be seen again full non-linear flame trajectories were only obtained over a limited range of equivalence ratio's namely; between Ø = 0.6 - 0.65 only.

Again present data for ethanol/air mixtures are compared against data from the literature presented by Holley et al. [8] in Fig. 5b.

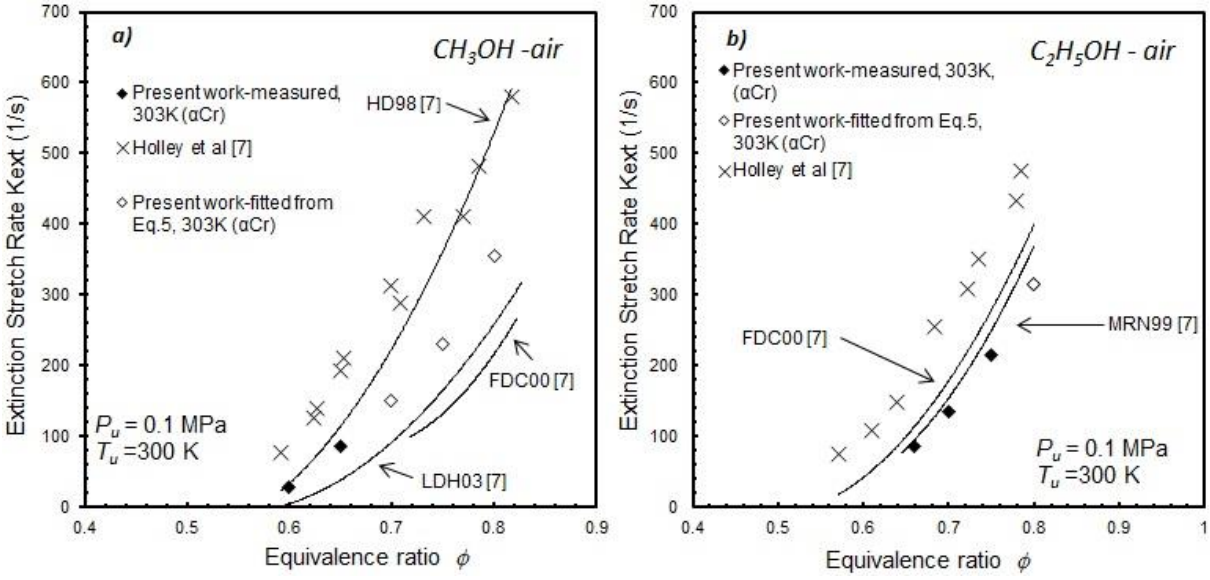

Figure 5. Comparison of experimental α_{Cr} against K_{ext} for a) lean CH_3OH/air and b) lean C_2H_5OH/air mixtures at 0.1 MPa and 300 K.

As in the case of methanol, values of K_{ext} obtained for ethanol/air mixtures increase as the mixture becomes richer, and again the data presented here are lower than the comparable data presented by Holley et al. [8], with again a similar offset of approximately 0.5 in equivalence ratio.

Encourangily, the gradients plotted between both alcohol datasets are for both cases similar, with, the current data comparing at least as or in some cases more favourably to the predictions from kinetic schemes FDC00 and MRN99.

It is now examine the percentage error deviation for the correlation between K_{ext} from the counter-flowing flames and the calculated α_{Cr} of all mixtures in Fig. 6. It can be seen that the vast majority of gaseous fuels data match the accuracy line well. However, the leanest CH_4/air and the richest C_3H_8/air mixtures are below 40% and above 10% from the accuracy line, respectively. This deviation is significantly important due to at these points the non-linear methodology to ignition energy is utilised to obtain the α_{Cr} value. Moreover, the discrepancies in the calculated α_{Cr} values are worst for all the fuel vapour data with an overall error of 40%. The next section will discuss these results in more detail.

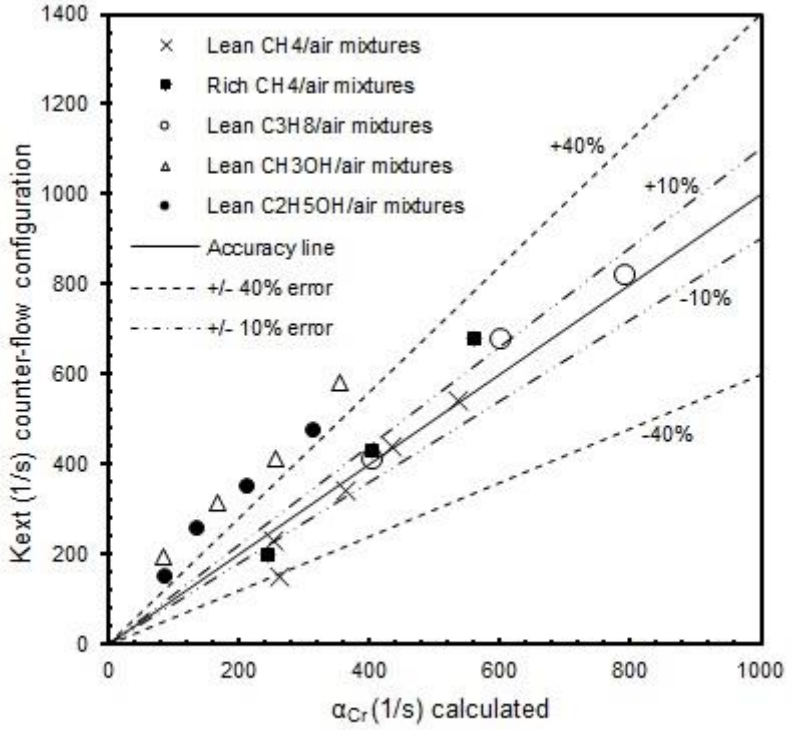

Figure 6. Percentage error deviation for the correlation between K_{ext} from the counter-flowing flames and the calculated α_{Cr} of all mixtures.

5. Discussion

The basic premise employed in this study concerns achieving minimal ignition energies, to reveal the sensitive early stages of flame front propagation, enabling the measurement or extrapolation of the critical stretch-rate so that it could be compared with the values of extinction strain rate quoted in the literature. Fig. 7a exemplifies the relationship between the Schlieren flame front radius (r_{sch}) and time, for the case of a weakly ignited lean ethanol/air mixture. In Fig. 7b propagation of a typical stretched flame is shown for the same dataset, revealing the non-linear flame speed characteristic.

As can be seen the development of the flame may be subdivided into three distinct regions (*A*, *B* and *C*) which allows for further discussion. In terms of stretch region *A* in Fig. 7b represents the spark driven zone, where the flame decelerates with increasing radius, hence both S_n and α are observed to decrease, in accordance with both deceleration and radius increase. This is understandable given the small, highly stretched flame kernel, surrounded by cold unburned reactant. Heat release from the spark must be sufficient to raise the thermal conduction in proportion to reactant mass diffusion, and generate enough heat to enable the flame to become self-propagating. Taking this to the limit, region *A* would not exist, with flame growth starting at the origin as determined by non-linear extrapolation equation (Fig. 2), though in practice this limit could never be realised. These observations support the conclusions of Kim et al. [16] with reduced excess enthalpy from the spark ignition energy, prior to the first turning point. If the critical value of ignition energy is not high enough the ignition kernel will extinguish.

Whilst attaining enough relative heat release to propagate, the flame kernel is initially small, and therefore reactant mass diffusion is still a dominant influence as the flame starts to accelerate. Hence, stretch rate rises with an increase in the velocity of propagation, as observed in region *B*. The flame eventually reaches a point where heat release and thermal conduction are in balance with the diffusivity of reactants entering the flame front. This point of apparent equi-diffusivity results in the critical turning point, denoted here as α_{Cr}, beyond which point the flame begins to accelerate with decreasing stretch. This explanation is supported by the work of Wu and Chen [34] who observed that extinction stretch rate K_{ext} decreases exponentially with *Le*. The authors conclude that strong spherical flames are observed in the region where *Le* is small, thus it is more difficult to extinguish the flame. The increased energy provides greater heat release in relation to mass diffusion, and hence the influential region *B* is lost. The same mechanism that controls flame extinction in the counter-flow technique through *Le*, is interpreted similarly by Law [35]. Again these observations support Kim et al. [16] conclusions about the self-sustained nature of the flame without assistance from the spark. However, the flame is relatively cold and strongly stretched due to the broadening of the reaction-diffusion zone, decreasing fuel diffusion to

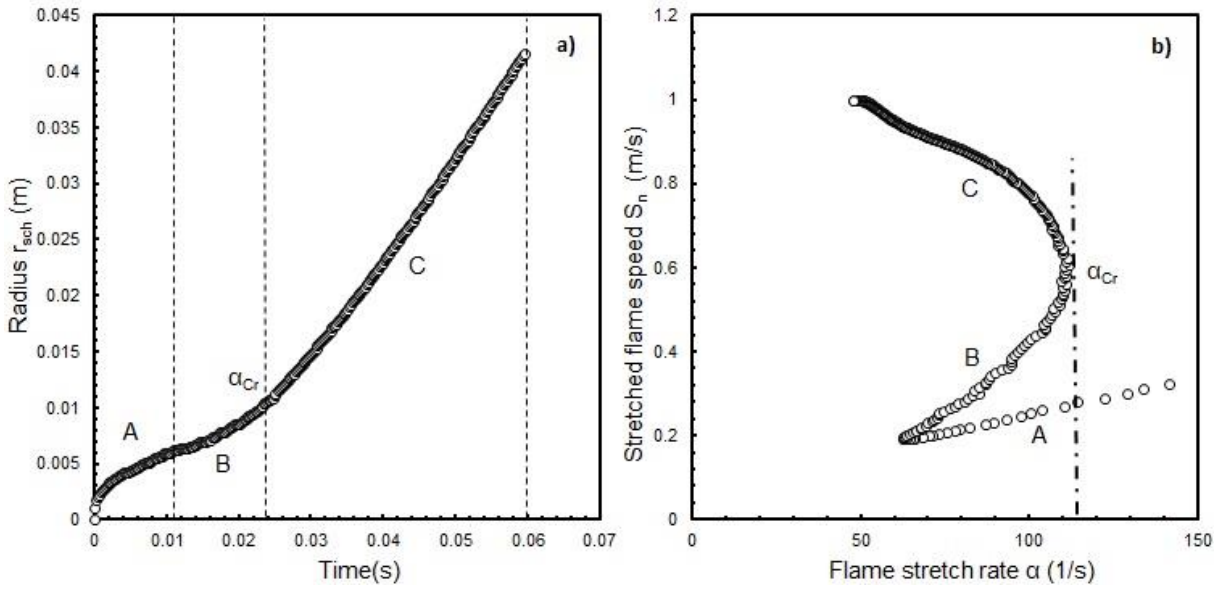

Figure 7. a) Relation between time after ignition and the Schlieren flame front radius (r_{sch}) and b) Flame propagation trajectory at low ignition energy for ethanol.

the reaction zone. Is at this turning point at which, according to Chen et al. [20], the critical Karlovitz number (*Ka*) have its maximum value. The *Ka* is given by $Ka = 2(S_n/S_L)\delta/r = \alpha\delta/u_L$, where δ is the

flame thickness. Therefore, as the authors stated, the flame speed reverse is caused by the substantial thickening of the flame initiated by the lowest ignition energy before it reaches the maximum *Ka*.

Moreover, in region *C* the traditional stretched flame propagation is identified, with greater heat release to the surrounding reactants lowering flame temperature and speed. This effect diminishes as curvature and stretch rate is reduced, and the flame front tends towards the planar limit, with flame speed correspondingly rising toward its unstretched limit. Hence it follows that the methodology presented can only be applied to self-sustaining stable reaction zones where *Le* >1.

Nonetheless, the data presented shows a partial correspondence between K_{ext} and $\alpha_{Cr,}$ quantitatively in the case of gaseous fuels. On the other hand, test undertaken with fuel vapour data presents an overall deviation of 40% with respect to the accuracy line. One explanation for this offset could be inaccuracies in equivalence ratio which are notoriously harder to control in the case of liquid vapours compared with gaseous fuels, due to issues with complete evaporation and potential 'dewing' out of liquid fuels on any surface that are cooler than the saturation temperature of the vapour in question, along with the fact that non-linear formulation is a simplified model which is derived based on several assumptions. Therefore, it is suggested the need for further investigation to clarify this behaviour.

Finally, it is informative to reconsider the evaluation of α_{Cr} presented in Fig. 7b and embedded within the non-linear extrapolation equation in light of the current dataset and proposed methodology. First, α (S_n) is taken as a function of S_n. Now α_{Cr}, defined as the critical turning point of α (S_n), may be determined explicitly via basic calculus. Hence, subject to the assumptions inherent in Eq.5, Eq.7 shows the critical stretch rate to be a function of laminar burning rate, density ratio and Markstein length.

$$\alpha_{Cr} = \frac{u_L}{2eL_b}\left(\frac{\rho_u}{\rho_b}\right) \tag{7}$$

6. Conclusions

A characterisation of critical stretch rate is appraised using an outwardly-propagating spherical flame configuration. Experiments conducted employing minimal ignition energy demonstrate how characteristics for propagating flames can be utilised to either measure directly or extrapolate the critical stretch rate.

The methodology established in the present work requires determination of the maximum value of stretch rate corresponding to the turning point of the non-linear relationship between S_n and α. However, a reduced dataset must be carefully selected to avoid data influenced by ignition or confinement, hence avoiding inaccurate evaluation of the unstretched flame speed.

When data is compared to previous studies using the traditional counter-flow technique, a partial correlation is obtained. Better agreement between the techniques is found for gaseous fuels compared with fuel vapour from two alcohols currently being proposed as alternative fuels, though the latter show similar trends and good agreement with chemical kinetic schemes. However, further investigation is needed to explain the offset between the results obtained in the present work, especially for the alcohols, and the experimentally determined counter-flow data.

Finally, a mathematical expression (Eq. 7) was produced to determine the critical stretch rate in terms of laminar burning rate, density ratio and Markstein length, applicable only at the specific conditions of the present work. Re-analysis of the underlying non-linear theory produce a similar profile for extinction stretch rate as a function of equivalence ratio for different fuels under fuel-lean conditions,

providing data for fire suppressant on premixed and non-premixed flames applications and an insight into the potential for fuel-flexibility in power generators such gas turbines and internal combustion engines by determining a wide range of operational conditions with high levels of combustion efficiency and for the validation of chemical kinetic mechanisms.

Acknowledgments

The authors acknowledge the financial support provided by the Mexican Council for Science and Technology (CONACYT), under the scholarship No. 309181.

Nomenclature

a	Thermal diffusivity, $m^2\ s^{-1}$	S_L	Unstretched flame speed, $m\ s^{-1}$
A	Area, m^2	S_n	Stretched flame speed, $m\ s^{-1}$
C	Capacitance, μF	T_u	Initial temperature, K
D	Mass diffusivity, $m^2\ s^{-1}$	u_L	Unstretched laminar burning velocity, $m\ s^{-1}$
E	Theoretical energy, mJ	V	Voltage, V
Ka	Karlovitz number		
K_{ext}	Extinction stretch rate, s^{-1}		*Greek symbols*
Le	Lewis number, (=a/D) [-]	α	Flame stretch rate, s^{-1}
L_u	Unburned Markstein length, m	α_{Cr}	Critical stretch rate, s^{-1}
L_b	Burned Markstein length, m	δ	Flame thickness, m
P_u	Initial pressure, Pa	Ø	Equivalence ratio, [-]
r_{sch}	Schlieren flame front radius, m	ρ_b	Density ratio of burned gases, $kg\ m^{-3}$
R	Wall radius, m	ρ_u	Density ratio of unburned gases, $kg\ m^{-3}$

References

[1] Choudhuri A.R., *et al*., Flame Extinction Limits of H2-CO Fuel Blends, *Journal of Engineering for Gas Turbines and Power, 130* (2008), 3, pp. 031501-031508.
[2] Park O., *et al*., Combustion characteristics of alternative gaseous fuels, *Proc. Combust. Inst. , 33* (2011), 1, pp. 887-894.
[3] Tomić M., *et al*., Closed Vessel Combustion Modelling by using Pressure-Time Evolution Function Derived from Two-Zonal Approach, *Thermal Science, 16* (2012), 2, pp. 561-572.
[4] Wang C.H., *et al*., The extinction limits and near-limits behaviors of premixed ethanol/air flame, *International Communications in Heat and Mass Transfer, 24* (1997), 5, pp. 695-708.
[5] Mansour M.S., Fundamental Study of Premixed Combustion Rates at Elevated Presure and Temperature, Ph. D. thesis, University of Leeds, UK, 2010.
[6] Lefebvre A.H., Ballal D.R., *Gas Turbine Combustion. Alternative Fuels and Emissions*, CRS Press, Taylor & Francis Group, Boca Raton, FL, USA, 2010.
[7] Geikie M.K., Ahmed K.A., Lagrangian mechanisms of flame extinction for lean turbulent premixed flames, *Fuel, 194* (2017), pp. 239-256.
[8] Holley A.T., *et al*., Extinction of premixed flames of practical liquid fuels: Experiments and simulations, *Combustion and Flame, 144* (2006), 3, pp. 448-460.
[9] Zhang Y., *et al*., Extinction limit and near-limit kinetics of lean premixed stretched H2-CO-air flames, *International Journal of Hydrogen Energy, 41* (2016), 39, pp. 17687-17694.
[10] Veloo P.S., Egolfopoulos F.N., Studies of n-propanol, iso-propanol, and propane flames, *Combustion and Flame, 158* (2011), 3, pp. 501-510.
[11] Ishizuka S., Law C.K., An experimental study on extinction and stability of stretched premixed flames, *Symposium (International) on Combustion, 19* (1982), 1, pp. 327-335.

[12] Xu W., Jiang Y., Qiu R., Ren X., Influence of halon replacements on laminar flame speeds and extinction limits of hydrocarbon flames, *Combustion and Flame*, *182* (2017) 1-13.
[13] Bradley D., *et al*., Explosion bomb measurements of ethanol-air laminar gaseous flame characteristics at pressures up to 1.4 MPa, *Combustion and Flame*, *156* (2009), 7, pp. 1462-1470.
[14] Crayford A.P., *et al*., Laminar Burning Characteristics of Methane/Water-Vapour/air Flames, *Proceedings*, European Combustion Meeting, Cardiff, UK, 2011, Vol. 1, pp. 1-6.
[15] Kelley A.P., Law C.K., Nonlinear effects in the extraction of laminar flame speeds from expanding spherical flames, *Combustion and Flame*, *156* (2009), 9, pp. 1844-1851.
[16] Kim H.H., *et al*., Measurements of the critical initiation radius and unsteady propagation of n-decane/air premixed flames, *Proc.Combust. Inst.*, *34* (2013), 1, pp. 929-936.
[17] De la Garza O.A., *et al*., Determination and introduction of the transport properties of soybean oil biodiesel in the CFD code OpenFOAM, *Thermal Science*, (2017 OnLine-First), doi. org/10.2298/TSCI170317157G.
[18] Ganji P.R., *et al.*, Computational Optimization of Biodiesel Combustion using Response Surface Methodology, *Thermal Science*, *21* (2017), 1B, pp. 465-473.
[19] Carrera J.L., *et al*., Numerical study on the combustion process of a biogas spark ignition engine, *Thermal Science*, *17* (2013), 1, pp. 241-254.
[20] Chen Z., *et al*., Effects of Lewis number and ignition energy on the determination of laminar flame speed using propagating spherical flames, *Proc. Combust. Inst.*, *32* (2009), 1, pp. 1253-1260.
[21] Chen Z., *et al*., On the critical flame radius and minimum ignition energy for spherical flame initiation, *Proc. Combust. Inst.*, *33* (2011), 1, pp. 1219-1226.
[22] Omari A., Tartakovsky L., Measurement of the laminar burning velocityusing the confined and unconfined spherical flame methods – A comparative analysis, *Combustion and Flame*, 168 (2016), pp. 127-137.
[23] Crayford A.P., Suppression of Methane-Air Explosions with Water in the form of 'Fine' Mists, Ph D. thesis, University of Wales, Cardiff, UK, 2004.
[24] Pugh D.G., *et al*., Parametric investigation of water loading on heavily carbonaceous syngases, *Combustion and Flame*, *164* (2016), pp. 126-136.
[25] Cameron L.R.J., Bowen P.J., Novel cloud chamber design for 'transition range' aerosol combustion studies, *Process Safety and Environmental Protection*, *79* (2001), 4, pp. 197-205.
[26] Rallis C.J., Garforth A.M., The determination of laminar burning velocity, Progress in Energy and *Combustion Science*, *6* (1980), 4, pp. 303-329.
[27] Bradley D., *et al*., The measurement of laminar burning velocities and Markstein numbers for iso-octane-air and iso-octane-n-heptane-air mixtures at elevated temperatures and pressures in an explosion bomb, *Combustion and Flame*, *115* (1998), 1-2, pp. 126-144.
[28] Lamoureux N., *et al*., Laminar flame velocity determination for H2-air-He-CO2 mixtures using the spherical bomb method, *Experimental Thermal and Fluid Science*, *27* (2003), 4, pp. 385-393.
[29] Giannakopoulos G.K., *et al.*, Consistent definitions of "Flame Displacement Speed" and "Markstein Length" for premixed flame propagation, *Combustion and Flame*, *162* (2015), 4, pp. 1249-1264.
[30] Xu C., *et al*., Laminar flame characteristcs of ethanol-air mixture: Experimental and simulation study, *Thermal Science*, (2017 OnLine-First), doi.org/10.2298/TSCI161001112X .
[31] Tahtouh T., *et al*., Measurement of laminar burning speeds and Markstein lengths using a novel methodology, *Combustion and Flame*, *156* (2009), 9, pp. 1735-1743.
[32] Bradley D., *et al*., Burning velocities, Markstein lengths, and flame quenching for spherical methane-air flames: A computational study, *Combustion and Flame*, *104* (1996), 1-2, 176-198.
[33] Egolfopoulos F.N., *et al*., Wall effects on the propagation and extinction of steady, strained, laminar premixed flames, *Combustion and Flame*, *109* (1997), 1-2, pp. 237-252.
[34] Wu Y.C., Chen Z., Asymptotic analysis of outwardly propagating spherical flames, *Acta Mechanica Sinica*, *28* (2012), 2, pp. 359-366.
[35] Law C.K., *Combustion Physics*, Cambridge University Press, New York, USA, 2006.